Fossil Record 28 (1) 2025, 67–77 | DOI 10.3897/fr.28.133743

PENSOFT

MUSEUM FÜR NATURKUNDE BERLIN

New data on the inner skull cavities of *Diplocynodon tormis* (Crocodylia, Diplocynodontinae) from the Duero Basin (Iberian Peninsula, Spain)

Alejandro Serrano-Martínez[1,2], Àngel H. Luján[1], Ángel García-Pérez[1], Josep Fortuny[1]

1 *Institut Català de Paleontologia Miquel Crusafont (ICP-CERCA), Universitat Autònoma de Barcelona, Edifici ICTA-ICP, c/ Columnes s/n, Campus de la UAB, 08193 Cerdanyola del Vallès, Barcelona, Spain*

2 *Facultad de Ciencias, Universidad Nacional de Educación a Distancia, Paseo Senda del Rey 9, Madrid, Spain*

https://zoobank.org/38C9F72B-C41A-4AA0-9399-511ACD90FFA9

Corresponding authors: Alejandro Serrano-Martínez (alejandro.serrano@icp.cat); Josep Fortuny (josep.fortuny@icp.cat)

Academic editor: Florian Witzmann ♦ **Received** 2 August 2024 ♦ **Accepted** 24 January 2025 ♦ **Published** 24 February 2025

Abstract

Inner skull cavities provide key characters to elucidate taxonomic, phylogenetic, and palaeobiological inferences in reptiles. Herein, an integral description of the extinct alligatoroid *Diplocynodon tormis* is presented based on its holotype, recovered from the Middle Eocene site of "Teso de la Flecha" (Salamanca, Spain). It is an almost complete skull only missing some bones of the posterior part of the basicranium. A computed tomography (CT-scan) allowed the creation of a 3D model that includes the paranasal air sinuses in association with the nasal cavity, the dorsal region of the forebrain, including the cerebral hemispheres and the olfactory tract and the bulbs, the maxillary and mandibular branches of the trigeminal nerve, and the nasopharyngeal duct. Based on this, an anatomical description is provided and compared with both extant and extinct members of Alligatoridae and Crocodyloidea, including the previously published neuroanatomical description of one of the paratypes of this species. Neurosensorial (such as olfactory ratio and visual acuity) and cognitive capabilities (such as Reptile Encephalization Quotient) were estimated for the holotype and paratype of *D. tormis* and compared to those of other crocodylians. The inner skull cavities of *D. tormis* are similar to those of other crocodylians. Interestingly, the polarity of some characters in their brain, paranasal sinuses, and pharyngotympanic sinus system support its position as a basal alligatoroid. Neurosensorial and cognitive estimations also concur with a medium-sized basal alligatoroid. Nonetheless, further studies including other fossil crocodylians are required to better understand the evolutionary patterns of the inner skull cavities that have been relevant during the evolution of this successful archosaurian lineage.

Key Words

Eocene, Europe, palaeoneurology, cranial endocast, Eusuchia

Introduction

Diplocynodon is a basal alligatoroid that inhabited Europe from the Late Palaeocene to the Middle Miocene (e.g., Hua 2004; Martin 2010a; Martin and Gross 2011; Delfino and Smith 2012; Martin et al. 2014; Chroust et al. 2019). Climatic deterioration that occurred during the Eocene–Oligocene transition (~33.9 Ma) negatively affected all crocodilian diversity, with *Diplocynodon* being the only surviving genus in Europe (Markwick 1998; Martin 2010b; Kotsakis et al. 2004; fosFARbase 2024). After the Middle Miocene Climatic Optimum, and more specifically during the Late Miocene, this genus was restricted to south European refuges until it became extinct due to a global cooling event (Böhme 2003; Delfino et al. 2007; Delfino and Rossi 2013).

To date, eleven species have been recognized, all of them endemic to Europe (Brochu 1999; Piras and Buscalioni 2006; Martin 2010a; Delfino and Smith 2012; Martin et al. 2014; Díaz Aráez et al. 2017; Luján et al.

2019; Macaluso et al. 2019; Rio et al. 2020; Massone and Böhme 2022; Venczel and Codrea 2022). As for the record of the Iberian Peninsula, three species have historically been recognized: *Diplocynodon tormis* from the Middle Eocene of the Duero Basin (Buscalioni et al. 1992); *Diplocynodon muelleri* from the Early Oligocene of the Ebro Basin (Kälin 1936; Piras and Buscalioni 2006); and *Diplocynodon ratelii* from the Early Miocene of the Vallès-Penedès Basin (Díaz Aráez et al. 2017). While its phylogenetic position is still debated, *Diplocynodon* is generally recovered at the base of Alligatoroidea, closely related to the basal alligatoroid genera *Deinosuchus* and *Leidyosuchus* (Brochu 1999; Delfino and Smith 2012; Martin et al. 2014; Groh et al. 2019; Macaluso et al. 2019; Rio et al. 2020; Massone and Böhme 2022).

Crocodyliform palaeobiodiversity recovered from the Duero Basin (Iberian Peninsula) is composed by *Iberosuchus* (a notosuchian) and three Crocodylian lineages: Planocraniidae (*Duerosuchus*), Alligatoroidea (*Diplocynodon*) and Crocodyloidea (*Asiatosuchus*) (Jiménez Fuentes 1974; Martín de Jesús et al. 1987; Buscalioni et al. 1992; Luis-Alonso and Luis-Alonso 2009; Fernández Díaz et al. 2013; Ortega et al. 2020; Narváez et al. 2021, 2024). Among them, *Diplocynodon* is the most abundant genus and *Diplocynodon tormis* (Buscalioni et al. 1992) was erected based on several specimens coming from the Middle Eocene of Areniscas de Cabrerizos Formation, Salamanca (Cuesta 1999; Fernández Díaz et al. 2013).

Regarding the neuroanatomy of fossil eusuchians, there has been a great increase in knowledge over the last few years (Barrios et al. 2023 and references therein). This is largely due to the improvement of non-invasive techniques, which have allowed the visualisation and reconstruction of the hard-to-observe inner bone (and specifically skull) cavities and greatly eased the handling and study thereof. Here we present a complete morphological description of the nasal cavity, paranasal sinuses, complete the neuroanatomical neurosensorial (olfactory ratio, visual acuity), and cognitive capabilities (Reptile Encephalization Quotient, REC) of *Diplocynodon tormis*, none of them described before for this species.

Material and methods

Studied material

Specimen IPS36361 (previously labelled as IPS9001 by Buscalioni et al. 1992) is the holotype of *Diplocynodon tormis* (Buscalioni et al. 1992). It is currently housed at the collections of the Institut Català de Paleontologia Miquel Crusafont (ICP) in Sabadell, Spain. It is a partial preserved skull, preserving most of the cranium and both mandibles (Fig. 1). The estimated skull length is 241 mm *sensu* Buscalioni et al. (1992). Some bones from the braincase and temporal region are missing, such as the supraoccipital, basioccipital, basisphenoid, quadrates, prootics, exoccipital, laterosphenoids, quadrates and quadratojugals, while others are partially preserved, such as the parietal, ectopterygoids, squamosals, and pterygoids. Moreover, the pterygoid is slightly damaged through its entire ventral surface and both jugals are misplaced. As for the lower jaw, both articulars and surangulars are also missing.

To create the three-dimensional (3D) endocast model, the specimen was scanned at the Hospital Universitari Mútua de Terrassa (Barcelona) using a standard X-ray CT system (model Sensations 16, Siemens). The parameters used were 140kV and 200 mA, obtaining a pixel resolution of 0.45 mm and 542 slices with an inter-slice of 0.5 mm. A sharpening process was performed to increase the contrast for a better identification of the structures with the software Avizo 7.1 standard edition, achieving a digital pixel resolution of 0.11 mm. The slices were segmented in Avizo 7.1 standard edition with semi-automatic tools to generate a model of the endocranial anatomy and related structures. The 3D model was post-processed, to smooth surfaces, fix mesh irregularities, and mirroring damaged regions from their homologous parts considering the plane of symmetry. Raw CT data and derived 3D models are available through MorphoSource. Herein we refer to the reconstructed cavities that house soft-tissue structures as if they were the structures themselves (e.g., "olfactory region" instead of "endocast of the olfactory region"). We follow the nomenclature by Dufeau and Witmer (2015) for cavities housed in the basicranium (brain and pharyngotympanic sinus system), and Witmer and Ridgely (2008) for the paranasal sinuses.

The previously described specimen STUS-344 (Serrano-Martínez et al. 2019a), a partial braincase designed as one of the paratypes of *D. tormis* (Buscalioni et al. 1992) and housed in the collection of the STUS at the Universidad de Salamanca (Spain), was also included to allow the posteriormost structures of the inner skull cavities to be studied. The inclusion of this specimen improves the comparative description of this species.

The inner skull cavities of both specimens assigned to *Diplocynodon tormis* (IPS36361 and STUS-344) were compared to those of all eusuchians for which inner cavities have been digitally reconstructed to date (Dufeau and Witmer 2007; Witmer and Ridgely 2008; Bona et al. 2013, 2017; Blanco et al. 2015; Brusatte et al. 2016; Serrano-Martínez et al. 2019a, 2019b, 2020; Kuzmin et al. 2021; Pochat-Cottilloux et al. 2022, 2023; Puértolas-Pascual et al. 2022, 2023; Barrios et al. 2023; Perrichon et al. 2023a, 2023b). However, for this study, we focused on including specimens for which 3D models of the inner skull cavities are available. Among basal Eusuchia, the allodaposuchids *Allodaposuchus subjuniperus* (MPZ 2012/288) and *Arenysuchus gascabadiolorum* (MPZ 2011/184) (Puértolas-Pascual et al. 2022), *Portugalosuchus azenhae* (ML1818) (Puértolas-Pascual et al. 2023), *Agaresuchus fontisensis* (HUE-2502) (Serrano-Martínez et al. 2020), and *Lohuecosuchus megadontos* (HUE-04498) (Serrano-Martínez et al. 2019b) were included in the comparative sample. Within

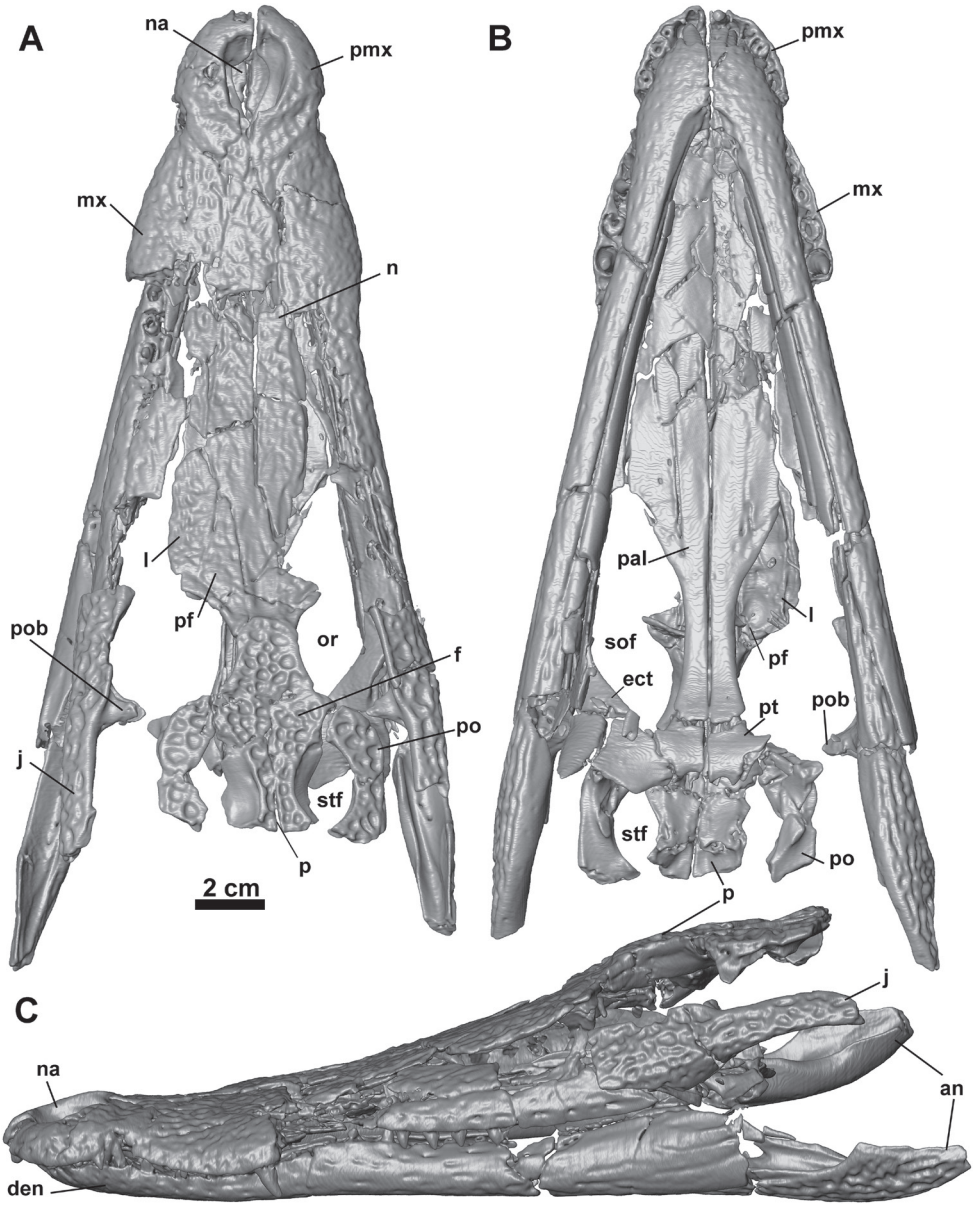

Figure 1. 3D model obtained of the skull of the holotype of *Diplocynodon tormis* IPS36361 in: **A.** Dorsal; **B.** Ventral; **C.** Left lateral views. Abbreviations: an, angular; den, dentary; ect, ectopterygoid; f, frontal; j, jugal; l, lacrimal; mx, maxilla; n, nasal; na, naris; p, parietal; pal, palatine; pf, prefrontal; pmx, premaxilla; po, postorbital; pob, postorbital bar; pt, pterygoid; or, orbit; stf, supratemporal fenestra; sof, suborbital fenestra.

the crown group Crocodylia, the comparative sample includes the paranasal sinuses, pharyngotympanic sinus system, the inner ear and the brain and related blood and nerve canals of the alligatorine *Alligator mississippiensis* (3D reconstruction based on MZB 92-0231) and the caimanines *Caiman crocodilus* and *Melanosuchus niger* (3D reconstruction based on IPS-D.135853 and RVC--JRH-FBC1, www.osf.io; respectively). Crocodyloidea is represented by *Crocodylus niloticus* (3D reconstruction based on MZB 2003-1423) and *Osteolaemus tetraspis* (reconstruction based on MZB 2006-0039). Lastly, digital reconstruction of the gavialoid *Gavialis gangeticus* (3D reconstruction based on UF118998, www.morphosource.org) and the phylogenetically unstable species *Tomistoma schlegelii* (3D reconstruction based on TMM M-6342, www.digimorph.org) completed the comparative sample. CT raw data and derived 3D models generated by the authors of this work are also available through MorphoSource. All in all, samples used in this study include animals of very different sizes. It has been shown that some characters may vary due to size and ontogeny (i.e. large individuals may present slightly marked transition through the olfactory tract and the cerebrum) (Dufeau and Witmer 2015). For this reason, results are shown taking into account the fact that size may affect some characters, as has been shown to happen in *Diplocynodon* (Serrano-Martínez et al. 2019a), and consequently the discussion takes this into account by referring to medium-sized or large-sized animals: Medium-sized specimens are defined as having a skull length (from the caudal edge of the supraoccipital to

the rostralmost tip of the premaxilla) between 100 and 300 mm. In our sample, this includes *C. crocodilus*, *O. tetraspis* and both *D. tormis*. We define large-sized animals as having a skull length larger than 300 mm, represented by *A. mississippiensis*, *C. niloticus*, *T. schlegelii*, *G. gangeticus*, *A. subjuniprus*, *A. gascabadiolorum*, *P. azenhae*, *A. fontisensis*, and *L. megadontos* in our sample.

Based on our available sample database, we performed estimations for the neurosensorial and cognitive capabilities of each analyzed specimen. The olfactory ratio was obtained by comparing the largest distance of the olfactory bulb and the cerebral hemispheres (in the studied samples, their widths), and then normalizing it with a log-transformation (Zelenitsky et al. 2009, 2011) For the visual acuity, relative volume of the optic lobe concerning the brain has been used when the eyeball or any preserved ocular structure isabsent (Martin et al. 2007; Torres and Clarke 2018). Finally, cognitive capabilities can be estimated via the Reptile Encephalization Quotient (REQ), an equation based on the volume of the brain endocast adjusted to the reptilian brain proportions (Hurlburt 1999). Body mass was estimated based on skull measurements (Dodson 1975; Webb and Messel 1978; Platt et al. 2011). Endocast volume was obtained using the measurement tool of Avizo Software. The endocast represents not only the brain, but also the dural envelope, a connective tissue that protects the brain. Brain/envelope proportion was described for a crocodylian ontogenetic series by Jirak and Janacek (2017) and Watanabe et al. (2018). These data were added into a regression formula that compares the endocast volume and the relative volume of the brain (fig. 5 from Serrano-Martínez et al. (2020)). Once the brain volume was estimated, brain mass was calculated assuming a density of 1 g/cm3 (Franzosa 2004).

Institutional abbreviations

HUE, Lo Hueco Collection, Museo de las Ciencias de Castilla-La Mancha (Cuenca, Spain); **IPS**, Institut Català de Paleontologia Miquel Crusafont, (formerly Institut de Paleontologia de Sabadell), Sabadell, Spain); **ML**, Museu da Lourinha (Lourinha, Portugal). **MPZ**, Museo Paleontológico de Zaragoza (Zaragoza, Spain). **MZB**, Museu de Ciències Naturals de Barcelona (Barcelona, Spain); **STUS**, Sala de las Tortugas "Emiliano Jiménez" de la Universidad de Salamanca (Salamanca, Spain); **TMM**, Texas Memorial Museum (Austin, USA). **UF**, University of Florida (Gainesville, USA).

Results

All preserved inner skull cavities of the specimen *Diplocynodon tormis* IPS36361 were 3D reconstructed (Figs 2, 3), showing the whole nasal sinuses and the anteriormost part of the brain including the dorsal region of the cerebral hemispheres and the olfactory bulbs and tracts. The other cavities are absent, due to the absence of the basisphenoid, occipital, prootic and pterygoids. A detailed description of the inner skull cavities of the paratype specimen STUS-344 was provided in Serrano-Martínez et al. (2019a) and is used here for comparisons.

Description

Nasal cavity and paranasal sinuses

Archosaurians have a very pneumatized skull, and the snout of crocodiles is a good example. Crocodilian anterior skull bones are full of recesses, which are part of the respiratory tract and are essential for the sense of smell (Witmer and Ridgely 2008). The principal of these cavities is the nasal airway, a long paired structure that crosses the skull anteroposteriorly, from the nares to the secondary choana, also opening to the olfactory region. The nasal airway is divided into the nasal passage, the anteriormost part, and nasopharyngeal ducts, which start just after the olfactory region opening (Fig. 2). Along the way, the nasal airway rises to several sinuses. The most remarkable of those sinuses are the antorbital sinus, postvestibular sinus and prefrontal sinus, which are related with other anatomical systems (Witmer and Ridgely 2008).

In *Diplocynodon tormis* IPS36361, the nares are almost enclosed by the premaxillae (Fig. 2A). They are subcircular and more elongated in the anteroposterior axis. The nares connect with the nasal passage, which is surrounded by the premaxillae anteriorly and the maxillae dorsolaterally. It runs anteroposteriorly from the nares, almost to the tip of the snout, to the secondary choanae, that open at the secondary palate ventrally to the basicranium. The nasal passage is connected to the paranasal sinuses ventrolaterally by a high number of openings, probably due to diagenetic breakages. The lateral limits of the nasal airway passage are almost straight in the anterior area, and widen posteriorly, approximately at the level of the midpart of this cavity, forming a large chamber. The olfactory region is one of the biggest chambers of IPS36361 (Fig. 2C). It is bilobate in shape and has a sagittal groove on its dorsal surface. The olfactory region is ventrally surrounded by the pterygoids, ventrolaterally by the maxillae, and dorsally by the lacrimals, prefrontals, nasals and frontals. The olfactory region of the nasal cavity contacts posterodorsally with the olfactory lobes, which continues by the olfactory tract to the rest of the brain, and ventrally with the nasopharyngeal ducts (Fig. 2D, E). Nasopharyngeal ducts are two parallel and posteroventrally oriented tubes. The boundary between the nasopharyngeal ducts and the olfactory region collapsed at some points, but the tubular structure of these ducts is easily distinguishable. Both nasopharyngeal ducts join in a common passage at the posteriormost region, just before opening in the secondary choana, which is not preserved in IPS36361.

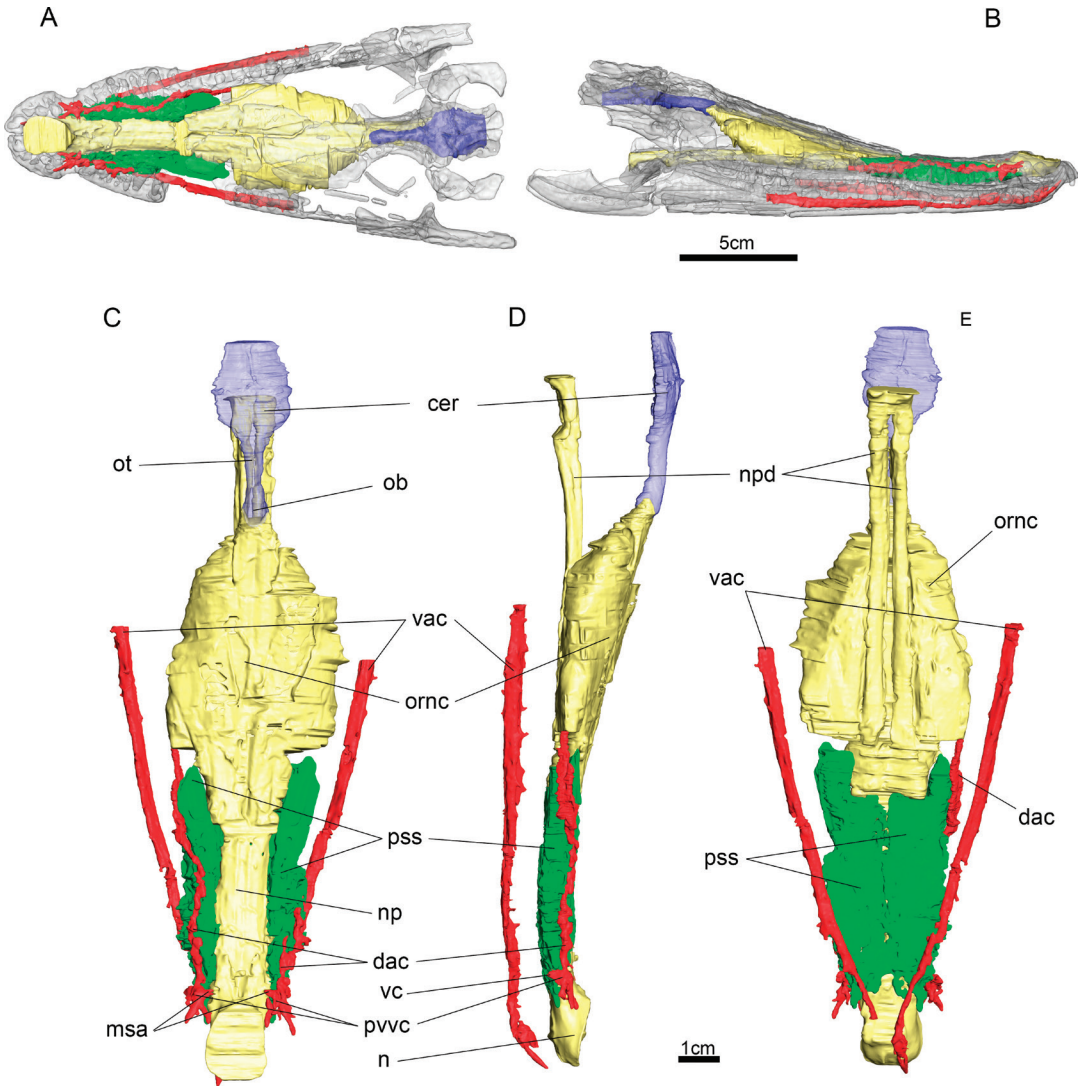

Figure 2. **A, B.** 3D model of the skull and inner skull cavities of the specimen *Diplocynodon tormis* IPS36361 in: **A.** Dorsal; **B.** Right lateral. Bone and brain were rendered semi-transparent. **C–E.** Inner cavities related with the nasal cavity, in **C.** Dorsal; **D.** Right lateral; **E.** Ventral. Abbreviations: cer, cerebral hemispheres; dac, dorsal alveolar canal; msa, medial subnarial anastomosis; n, naris; np, nasal passage; npd, nasophryngeal duct; ob, olfactory bulb; ornc, olfactory region of the nasal cavity; ot, olfactory tract; pss, paranasal sinus system; pvvc, paravestibular vascular bundle; vac, ventral alveolar canal; vc, ventral canal of the paravestibular vascular bundle.

As for the paranasal sinus system, it is difficult to assess with confidence the boundaries between the postvestibular and the antorbital sinuses. Therefore, both chambers are described together. The paranasal sinuses are located in the snout, lateral and ventral to the nasal airway passage, between the nares and the ofactory region of the nasal cavity (Fig. 2). They are composed of a complex of diverticula enclosed by the maxillae, and laterally limited by the tooth alveoli.

The dorsal alveolar canal is a bony neurovascular canal that houses the maxillary branch of the trigeminal nerve (V_2). It is anteroposteriorly oriented and located laterally and parallel to the paranasal sinus system. It connects with the nasal cavity via medial subnarial anastomosis, which emerges from the paravestibular vascular bundle. From this bundle also emerges a ventral canal that opens on the palate between the third and the fourth maxillary tooth. Only the right dorsal alveolar canal preserves the posterior region of the canal, which opens at the olfactory region of the nasal cavity. The ventral alveolar canal, which houses the mandibular branch of the trigeminal (V_3), crosses the dentaries longitudinally, close and ventrolaterally to the mandibular tooth alveoli (Fig. 2B, D)

Brain and pharyngotympanic sinus system

IPS36361 lacks most of the occipital region and only the anterior portion of the parietal and the postorbitals are preserved in anatomical connection with the skull (Fig. 1A, B). Hence, the hindbrain and the ventral part of the brain, cannot be reconstructed. However, the dorsal part of the cerebrum, in contact with the parietal and both frontals and prefrontals, is well preserved (Fig. 3). It allows the dorsolateral parts of the cerebral hemispheres to be determined. The anteriormost part of the forebrain is formed by the olfactory bulbs. They are a bilobate structure with a sagittal groove-like

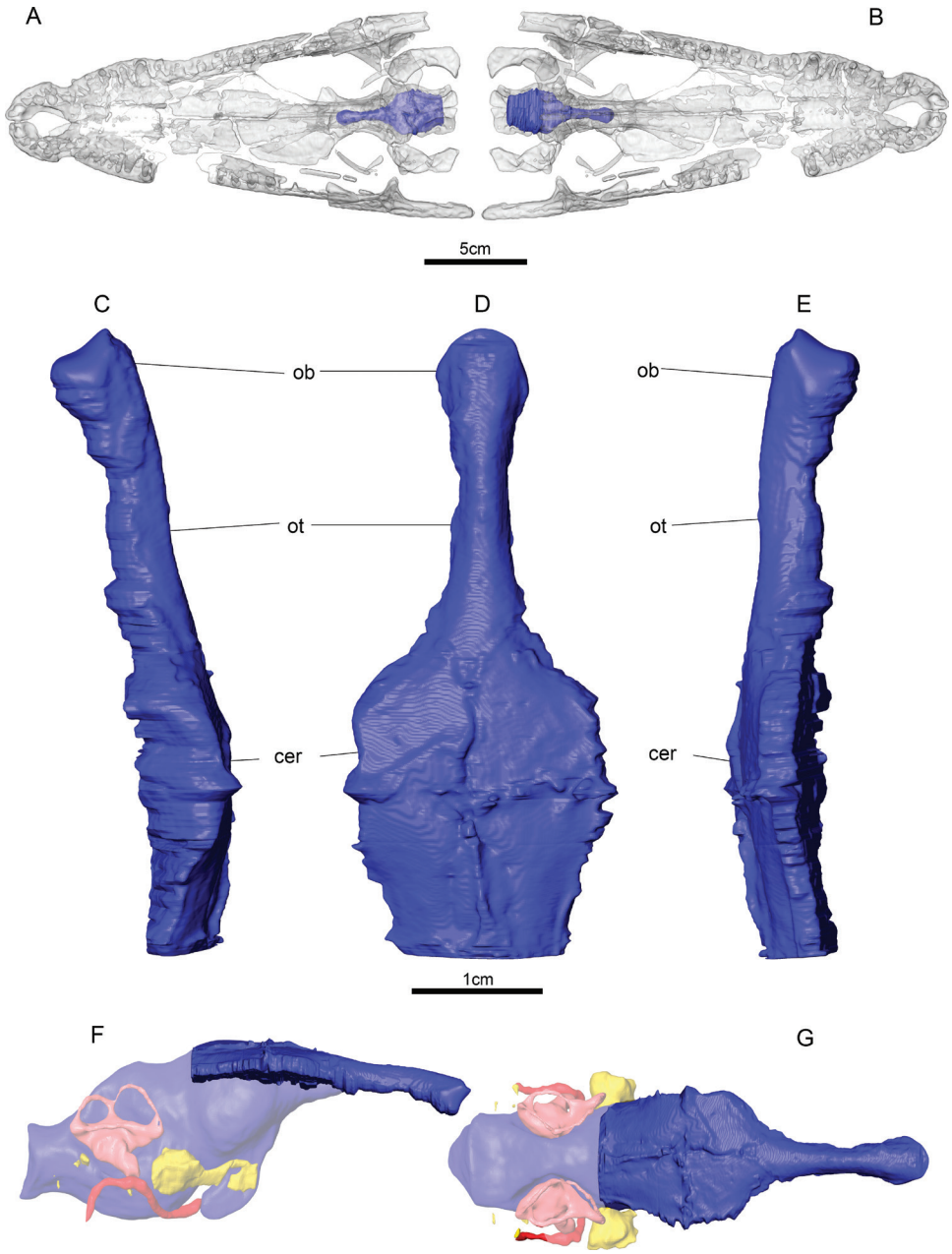

Figure 3. **A, B.** 3D model obtained of the inner skull cavities of *Diplocynodon tormis* IPS36361, focusing on the brain in: **A.** Dorsal; **B.** Ventral. Skull was rendered semi-transparent. **C–E.** Endocast of the brain in **C.** Left lateral; **D.** Dorsal; **E.** Right lateral. **F, G.** Idealized complete *Diplocynodon tormis* endocast based on IPS36361 brain overlapped on *Caiman crocodilus* IPS-D.135853 semitransparent endocast; **F.** Right lateral; **G.** Dorsal. Abbreviations: cer: cerebral hemispheres; ob, olfactory bulb; ot, olfactory tract.

mark in the dorsal part (Fig. 3C). The bulb is connected posteriorly with the rest of the brain by a long tube referred to as the olfactory tract. The olfactory tract widens before reaching the cerebrum. Both cerebral hemispheres are well preserved. In dorsal view, the cerebral hemispheres are distinguishable as two rounded lumps (Fig. 3C). The absence of the hindbrain in IPS36361 impedes determining whether the cerebrum is sigmoidal shaped in lateral view, as in STUS-344 (Serrano-Martínez et al. 2019a) and all the other crocodylians (Barrios et al. 2023).

The pharyngotympanic sinus system in crocodiles is constituted by a complex middle ear-diverticula around the hindbrain, but IPS36361 lacks this whole area.

Endocranial sensory system of *Diplocynodon tormis*

Three-dimensional reconstructions of the inner skull cavities allow their morphological description, but also enable estimates of the neurosensorial and cognitive capabilities by studying the structures that housed these sensory organs. The partial preservation of IPS36361 only allowed the olfactory capability of the specimen to be analysed. On the other hand, 3D reconstruction of STUS-344 allows the olfactory, visual, and cognitive capabilities to be estimated. The absence of the inner ear in both specimens impedes any study of the hearing in this species.

The relative size of the olfactory bulb is related to the number and size of mitral cells and the number of smell receptors and olfactory receptor genes, and therefore, to the olfactory acuity (Zelenitsky et al. 2009, 2011 and references therein). The results of Zelenitsky et al. (2009) show that crocodylians have a high olfactory ratio, which agrees with their acute olfactory sense (Weldon et al. 1990; Weldon and Ferguson 1993). Our results are similar to those reported by Zelenitsky as the *Alligator mississippiensis* specimen here analysed presents an olfactory ratio of 1.76, close to the range assigned for this taxon (1.70–1.74) by (Zelenitsky et al. 2009). The other comparative samples herein analysed have ratios between 1.69–1.82. Crocodyloids (1.79–1.82) have higher olfactory ratios than alligatoroids (1.68–1.76), independently of their size (Table 1) while the olfactory ratio estimated for the *D. tormis* paratype, STUS-344, is 1.76, within the expected range for alligatoroids while the ratio obtained for the holotype, IPS36361, is 1.64, a bit lower than other alligatoroids.

Table 1. Measurements for the olfactory capability calculations, based on Zelenitsky et al. (2009, 2011).

Taxon	Olfactory bulb (mm)	Cerebral hemispheres (mm)	Log olfactory ratio
A. mississippiensis	17.30	29.80	**1.76**
M. niger	13.95	28.73	**1.69**
C. crocodilus	10.92	19.62	**1.75**
C. niloticus	20.37	30.50	**1.82**
O. tetraspis	15.43	24.90	**1.79**
T. schlegelii	19.13	28.89	**1.82**
G. gangeticus	16.65	33.29	**1.70**
D. tormis STUS-344	12.14	21.30	**1.76**
D. tormis IPS36361	8.15	18.53	**1.64**

Visual acuity is related to the size of the eyeball in vertebrates (Hall and Ross 2007; Hall 2008, 2009; Schmitz 2009). However, these structures are not preserved, and there are no studies relating the ocular orbit and the size of the eyeball in crocodiles.

Alternatively, the optic lobe is an easily recognizable area in crocodylians (Jirak and Janacek 2017), and its relative volume can be used as a proxy for optic capabilities, as in birds (Martin et al. 2007; Torres and Clarke 2018). The relative volume of the optic lobe concerning the brain is between 10 and 15% in the large-sized samples, and between 19 and 22% in the medium-sized ones (Table 2). STUS-344, a medium-sized animal, has a relative volume of the optic lobe of 16%, being lower compared to other specimens of similar size.

Cognitive capabilities are usually estimated by calculating the Reptile Encephalization Quotient (REQ). Crocodylian REQ is between 0.96 and 1.71 in analysed specimens (Table 3). The medium-sized specimens *Osteolaemus tetraspis* and *Caiman crocodilus* herein analysed have the highest REQs values, while the range of analysed large-sized specimens present values ranging from 0.9 to 1.2 (except for *Melanosuchus niger*, although it does not reach the REQs of those of medium-sized samples). The REQ of *D. tormis* STUS-344 is 1.13, within the obtained crocodylian range, but low compared with the other medium-sized specimens.

Table 2. Measurements for the relative size of the optic region, based on Jirak and Janacek (2017).

Taxon	Endocast volume (mm^3)	Optic lobe volume (mm^3)	Relative Volume
A. mississippiensis	18719.90	2467.94	**0.13**
M. niger	24001.20	4447.06	**0.19**
C. crocodilus	4941.74	936.48	**0.19**
C. niloticus	24764.80	3789.03	**0.15**
O. tetraspis	11593.10	2577.36	**0.22**
T. schlegelii	19390.50	2105.72	**0.11**
G. gangeticus	38309.90	6996.52	**0.18**
D. tormis STUS-344	7000.33	1149.00	**0.16**

Table 3. Measurements for the Reptile Encephalization Quotient calculations, based on Hurlburt et al. (2003).

Taxon	Endocast volume (cm^3)	Brain volume* (cm^3)	Body mass (g)	REQ
A. mississippiensis	18.72	6.91	104328.28[1]	**0.96**
M. niger	24.00	8.20	59108.00[1]	**1.55**
C. crocodilus	4.94	2.75	5887.67[1]	**1.71**
C. niloticus	24.76	8.38	151389.30[2]	**0.96**
O. tetraspis	11.59	4.96	20228.39[2]	**1.63**
T. schlegelii	19.39	7.08	93619.60[3]	**1.04**
G. gangeticus	38.31	11.32	170000**	**1.23**
D. tormis STUS-344	70.00	3.50	20885.51[1]	**1.12**

*The brain volume was estimated by introducing the data of Jirak and Janacek (2017) and Watanabe et al. (2018) in a regression plot (Fig. 4). The body mass was estimated using skull measurements, based on [1]Dodson (1975); [2]Webb and Messel (1978); [3]Platt et al. (2011).
**average species body mass.

Discussion

Cladistic analyses place the genus *Diplocynodon* as a basal member of Alligatoroidea (Brochu 1999; Piras and Buscalioni 2006; Delfino and Smith 2012; Martin et al. 2014; Groh et al. 2019; Macaluso et al. 2019; Rio et al. 2020), and its brain shape reinforces this hypothesis, showing a mosaic of crocodylian plesiomorphies and alligatoroid synapomorphies (Serrano-Martínez et al. 2019a). The inclusion of IPS36361 allows us to confirm that the paranasal sinus cavities, undescribed for this species, are also similar to those of other alligatoroids.

The nares of *Diplocynodon tormis* are subcircular in shape, fully enclosed within the premaxilla. As in most crocodylians, bony openings of the rostrils are not divided into two due to the projection of the nasals to join the premaxilla (Brochu 1999). The nasal passage and olfactory region of *D. tormis* are similar to those of other eusuchians (Fig. 4). Nasopharyngeal ducts have horizontal orientation in lateral view, as other crocodylians (Fig. 4). Specifically, the nasopharyngeal ducts of *D. tormis* and *C. crocodilus* have the same shape and orientation (Fig. 4). They usually

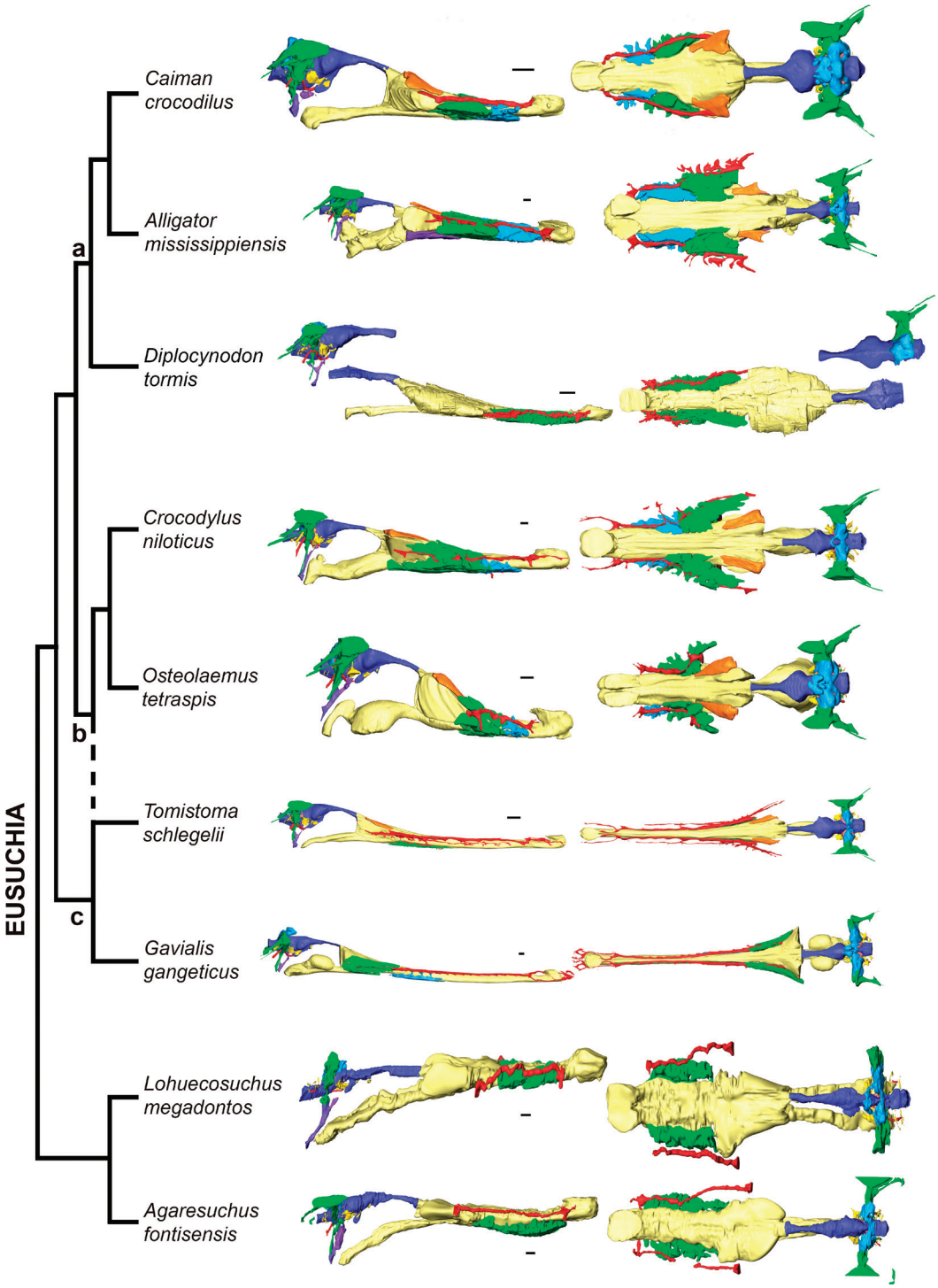

Figure 4. IPS36361 and STUS-344 reconstructions compared to those of other crocodylians described by Serrano-Martínez et al. (2019a, 2019b, 2020). Scale bars: 1 cm.

continue into an abrupt 90° ventral turn in crocodylians, just before opening into the internal choana (Puértolas-Pascual et al. 2022, 2023; Serrano-Martínez et al. 2019b, 2020), but this section of the ducts is missing.

Paranasal air sinuses of IPS36361 are similar to those of other eusuchians. Although the breakage of several septs impedes a rigorous comparison, the right dorsal alveolar canal is complete and its posteriormost part opens in the olfactory region of the nasal cavity, as described for alligatoroids in Serrano-Martínez et al. (2019b, 2020).

The only regions preserved in IPS36361 are the dorsal parts of the forebrain (including the tracts and olfactory bulbs). These regions were already described in STUS-344 (Serrano-Martínez et al. 2019a), and both specimens have the same morphology: rounded cerebral hemispheres and abrupt transition with the olfactory tract in dorsal view (Fig. 4). This morphology is also present in other specimens from the medium-sized sample, such as *Caiman crocodilus*, *Osteolaemus tetraspis* or juvenile of *Alligator mississippiensis* (Serrano-Martínez et al. 2019a).

Neurosensory capabilities in diplocynodontids

Zelenitzsky studied the olfactory capabilities of birds and non-avian dinosaurs (Zelenitsky et al. 2009, 2011), and demonstrated the large relative size of the olfactory bulbs of *A. mississippiensis* in comparison to other archosaurs. Crocodylians here studied seem to have similar olfactory acuity than that of *A. mississippiensis* analyzed by Zelenitsky et al. (2009). The olfactory acuity estimated for STUS-344 (1.76) is close to those of other studied alligatoroids (1.69–1.76), and far enough from those of crocodyloids (1.79–1.82). IPS36361 has an olfactory ratio lower than those of other alligatoroids (1.64), but is closer to alligatoroids than to crocodyloids. However, we must consider that the measurement of the brain hemispheres cannot be as precise as required due to the partial preservation of this region. Regardless, these values are compatible with the hypothesis that the relative size of the olfactory bulb has a stronger phylogenetical signal than the size of the specimen (Serrano-Martínez et al. 2019b, 2020).

The cognitive capabilities of crocodylians and other non-avian reptiles are less developed than those of mammals and birds (Jerison 1969, 1973; Grigg and Kirshner 2015). The Reptile Encephalization Quotient (REQ) takes into account turtles, lepidosaurs and crocodiles, and varies in a range between 0.4 and 2.4. Specifically, crocodylian REQ is between 0.9 and 1.5 (Hurlburt 1996; table 3). The encephalization quotient of crocodylians seems to be correlated with the ontogenetic state (Watanabe et al. 2018; Hu et al. 2021), and/or the size of the specimens (Serrano-Martínez et al. 2019b, 2020; Puértolas-Pascual et al. 2022, 2023), rather than their phylogenetic position. However, *D. tormis'* REQ is lower than those of the medium-sized crocodylians (Table 3), and more similar to that of the large-sized ones. This implies that the cognitive capabilities of *D. tormis* are less developed than the average for its size. It should be kept in mind, however, that these results may not be as accurate as expected, due to the breakages of the otic capsules and the anteroventral part of the laterosphenoids. As such, additional specimens of this taxon are needed to further evaluate the Encephalization Quotient of this species

Conclusions

Since the application of CT methodologies in vertebrate palaeontology, its use for deciphering neuroanatomy has become generalized. Crocodiles and related forms are one of the groups that saw a large increase in studies using CT raw data and derived 3D models to provide novel information on inner skull cavities. In the present study on *D. tormis*, the 3D model works as a support for the morphological description of the nares, nasal passage, olfactory region, nasopharyngeal duct and all associated air sinuses, never described before for this species. Comparing this description with extant members of Crocodylia, and specifically with the Alligatoridae family, provides evidence supporting the placement of *D. tormis* as a basal alligatoroid. Supplementing the description, neurosensory estimations such as an acute but not as sharp as crocodyloid olfactory acuity (with 1.76 and 1.64 olfactory ratios for the paratype and holotype of *D. tormis*, respectively) further support the position of *D. tormis* as a basal alligatoroid, while its visual acuity and cognitive capabilities (with a REQ value of 1.12 for the paratype of *D. tormis*) place it at a midpoint between the large-sized and medium-sized crocodylians.

Data archiving statement

CT-scans raw data and derived 3D models are available in Morphosource: CT raw data is available upon request for research purposes following the same guidelines as for physical fossils housed in the ICP while 3D models are openly available (https://www.morphosource.org/projects/000650843?locale=en).

Acknowledgements

This work was supported by the CERCA programme (ICP) from the Generalitat de Catalunya and the research projects PID2020-117118GB-I00 (to A.S.M. and J.F.) and PID2020-117289GB-I00 (to À.H.L.) funded by MCIN/AEI/10.13039/501100011033. J.F. is member of the consolidated research group (GRC) 2021 SGR 01184, whereas À.H.L is member of the consolidated research group (GRC) 2021 SGR 01192. This work is part of the Ramon y Cajal grant to J.F. [RYC2021-032857-I] financed by MCIN/AEI/10.13039/501100011033 and the European Union "NextGenerationEU" / PRTR. À.H.L. acknowledges the 'Programa Postdoctoral Beatriu de Pinós de la Secretaria d'Universitats i Recerca del Departament d'Empresa i Coneixement de la Generalitat de Catalunya' (2019 BP 00154). We thank Hospital Universitari Mútua de Terrassa, and CT technician A. López-García, for scanning the specimen IPS36361 and S. Llácer (ICP) for pre-process and assistance during the CT-scan process. We acknowledge Centre de Recuperació d'Amfibis i Rèptils de Catalunya (A. Martínez-Silvestre) and Museu de Ciències Naturals de Barcelona (J. Quesada) for comparison specimens used in this study. We greatly acknowledge helpful reviews of Prof. Paula Bona and one anonymous reviewer as well as Editor suggestions. Last, but not least, we thank D. P. Groenewald for proofreading the manuscript.

References

Barrios F, Bona P, Paulina-Carabajal A, Leardi JM, Holliday CM, Lessner EJ (2023) An overview on the Crodylomorpha Cranial Neuroanatomy. In: Paleoneurology of Amniotes. Springer, 213–266, https://doi.org/10.1007/978-3-031-13983-3

Böhme M (2003) The Miocene Climatic Optimum: evidence from ectothermic vertebrates of Central Europe. Palaeogeography Palaeoclimatology Palaeoecology 195: 389–401. https://doi.org/10.1016/S0031-0182(03)00367-5

fosFARbase (2024) fosFARbase. www.wahre-staerke.com

Brochu CA (1999) Phylogenetics, taxonomy, and historical biogeography of Alligatoroidea. Journal of Vertebrate Paleontology 19: 9–100. https://doi.org/10.1080/02724634.1999.10011201

Buscalioni ÁD, Sanz JL, Casanovas ML (1992) A new species of the eusuchian crocodile *Diplocynodon* from the Eocene of Spain. Neues Jahrbuch für Geologie und Paläontologie Abhandlungen 187: 1–29. https://doi.org/10.1127/njgpa/187/1992/1

Chroust M, Mazuch M, Luján ÀH (2019) New crocodilian material from the Eocene-Oligocene transition of the NW Bohemia (Czech Republic): an updated of fossil record in Central Europe during the Gran Coupure. Neues Jahrbuch für Geologie und Paläontologie Abhandlungen 293: 73–82. https://doi.org/10.1127/njgpa/2019/0832

Cuesta MA (1999) Las faunas de mamíferos del Eoceno de la Cuenca del Duero (Castilla y León, España). Síntesis bioestratigráfica y biogeográfica. Revista Española de Paleontología 14: 203–216. https://doi.org/10.7203/sjp.23781

Delfino M, Rossi MA (2013) Fossil crocodylid remains from Scontrone (Tortonian, southern Italy) and the Late Neogene Mediterranean biogeography of crocodylians. Geobios 46: 25–31. https://doi.org/10.1016/j.geobios.2012.10.006

Delfino M, Smith T (2012) Reappraisal of the morphology and phylogenetic relationships of the middle Eocene alligatoroid *Diplocynodon deponiae* (Frey, Laemmert, and Riess, 1987) based on a three-dimensional specimen. Journal of Vertebrate Paleontology 32: 1358–1369. https://doi.org/10.1080/02724634.2012.699484

Delfino M, Böhme M, Rook L (2007) First European evidence for transcontinental dispersal of *Crocodylus* (Late Neogene of southern Italy). Zoological Journal of the Linnean Society 149: 293–307. https://doi.org/10.1111/j.1096-3642.2007.00248.x

Díaz Aráez JL, Delfino M, Luján ÀH, Fortuny J, Bernardini F, Alba DM (2017) New remains of *Diplocynodon* (Crocodylia: Diplocynodontidae) from the Early Miocene of the Iberian Peninsula, Comptes Rendus Palevol 16: 12–26. https://doi.org/10.1016/j.crpv.2015.11.003

Dodson P (1975) Functional and ecological significance of relative growth in *Alligator*. Journal of Zoology 175: 315–355. https://doi.org/10.1111/j.1469-7998.1975.tb01405.x

Fernández Díaz PR, Alonso Gavilán G, Jiménez Fuentes E, Martín de Jesús S (2013) Análisis preliminar de un nuevo yacimiento de vertebrados fósiles (Arenal del Ángel-3), Eoceno Medio, Formación Areniscas de cabrerizos (Salamanca, España): Estratigrafía y contenido paleontológico. Studia Geologica Salmanticensia 49: 135–155.

Franzosa JW (2004) Evolution of the brain in Theropoda (Dinosauria). Thesis Dissertation, University of Texas at Austin, USA, 357 pp.

Grigg GC, Kirshner D (2015) Biology and Evolution of Crocodylians. Cornell University Press, Ithaca, New York, 650 pp. https://doi.org/10.1146/annurev.ento.52.110405.091303

Groh S, Upchurch P, Barrett PM, Day JJ (2019) The phylogenetic relationships of neosuchian crocodiles and their implications for the convergent evolution of the longirostrine condition. Zoological Journal of Linnean Society 188: 473–506. https://doi.org/10.1093/zoolinnean/zlz117

Hall MI (2008) The anatomical relationships between the avian eye, orbit and sclerotic ring: Implications for inferring activity patterns in extinct birds. Journal of Anatomy 212: 781–794. https://doi.org/10.1111/j.1469-7580.2008.00897.x

Hall MI (2009) The relationship between the lizard eye and associated bony features: A cautionary note for interpreting fossil activity patterns. Anatomical Record 292: 798–812. https://doi.org/10.1002/ar.20889

Hall MI, Ross CF (2007) Eye shape and activity pattern in birds. Journal of Zoology 271: 437–444. https://doi.org/10.1111/j.1469-7998.2006.00227.x

Hu K, King JL, Romick CA, Dufeau DL, Witmer LM, Stubbs TL, Rayfield EJ, Benton MJ (2021) Ontogenetic endocranial shape change in alligators and ostriches and implications for the development of the non-avian dinosaur endocranium. Anatomical Record 304: 1759–1775. https://doi.org/10.1002/ar.24579

Hua S (2004) Les crocodiliens du Sparnacien (Eocène inférieur) du Quesnoy (Oise, France). Oryctos 5: 57–62.

Hurlburt GR (1996) Relative brain size in recent and fossil amniotes: determination and interpretation. PhD Dissertation. Department of Zoology. University of Toronto, Toronto, 253 pp.

Hurlburt GR (1999) Comparison of body mass estimation techniques, using Recent reptiles and the pelycosaur *Edaphosaurus boanerges*. Journal of Vertebrate Paleontology 19: 338–350. https://doi.org/10.1080/02724634.1999.10011145

Hurlburt GR, Heckert AB, Farlow JO (2003) Body mass estimates of phytosaurs (Archosauria: Parasuchidae) from the Petrified Forest Formation (Chinle Group: Revueltian) based on skull and limb bone measurements. New Mexico Museum of Natural History and Science Bulletin 24: 105–113.

Jerison HJ (1969) Brain evolution and dinosaur brains. The American Naturalist 103: 575–588. https://doi.org/10.1086/282627

Jerison HJ (1973) Evolution of the brain and intelligence. Academic Press, New York and London, 482 pp. https://doi.org/10.1016/B978-0-12-385250-2.50018-3

Jiménez Fuentes E (1974) Iniciación al estudio de la climatología del Paleógeno de la Cuenca del Duero y su posible relación con el resto de la Península Ibérica. Boletín Geológico y Minero 85: 518–524.

Jirak D, Janacek J (2017) Volume of the crocodilian brain and endocast during ontogeny. PLoS ONE 12: e0178491. https://doi.org/10.1371/journal.pone.0178491

Kälin JA (1936) *Hispanochampsa mülleri* nov. gen. nov. spec., einneuer Crocodilidea usdemunteren Oligocaenvon Tárrega (Catalonien), Abhandlungen Schweizerischen Palaeontologischen 58: 1–40.

Kotsakis T, Delfino M, Piras P (2004) Italian Cenozoic crocodilians: taxa, timing and palaeobiogeographic implications. Palaeogeography Palaeoclimatology Palaeoecology 210: 67–87. https://doi.org/10.1016/j.palaeo.2004.03.013

Luis-Alonso S, Luis-Alonso A (2009) Nuevo género de Crocodylia del Eoceno medio de la Península Ibérica (Zamora, España): *Duerosuchus piscator* nov. gen., nov. sp. Studia Geologica Salmanticensia 45: 149–173.

Luján ÀH, Chroust M, Černansky A, Fortuny J, Mazuch M, Ivanov M (2019) First record of *Diplocynodon ratelii* Pomel, 1847 from the early Miocene site of Tušimice (Most Basin, Northwest Bohemia, Czech Republic). Comptes Rendus Palevol 18: 877–889. https://doi.org/10.1016/j.crpv.2019.04.002

Macaluso L, Martin JE, Favero LDEL, Delfino M (2019) Revision of the crocodilians from the Oligocene of Monteviale, Italy, and the diversity of European eusuchians across the Eocene-Oligocene boundary. Journal of Vertebrate Paleontology 39: e1601098. https://doi.org/10.1080/02724634.2019.1601098

Markwick PJ (1998) Crocodilian diversity in space and time: the role of climate in paleoecology and its implication for understanding

K/T extinctions. Paleobiology 24: 470–497. https://doi.org/10.1017/S009483730002011X

Martín de Jesús S, Jiménez Fuentes E, Fincias B, del Prado JM, Mulas Alonso E (1987) Los crocodylia del Eoceno y Oligoceno de la Cuenca del Duero. Dientes y osteodermos. Revista Española de Paleontolpgía 2: 95–108. https://doi.org/10.7203/sjp.25220

Martin GR, Wilson KJ, Wild JM, Parsons S, Kubke MF, Corfield J (2007) Kiwi forego vision in the guidance of their nocturnal activities. PLoS ONE 2(2): e198. https://doi.org/10.1371/journal.pone.0000198

Martin JE (2010a) A new species of *Diplocynodon* (Crocodylia, Alligatoroidea) from the Late Eocene of the Massif Central, France, and the evolution of the genus in the climatic context of the Late Palaeogene. Geological Magazine 147: 596–610. https://doi.org/10.1017/S0016756809990161

Martin JE (2010b) *Allodaposuchus* Nopsca, 1928 (Crocodylia, Eusuchia), from the Late Cretaceous of southern France and its relationships to Alligatoroidea. Journal of Vertebrate Paleontology 30: 756–767. https://doi.org/10.1080/02724631003758318

Martin JE, Gross M (2011) Taxonomic clarification of *Diplocynodon* Pomel, 1847 (Crocodylia) from the Miocene of Styria, Austria. Neues Jahrbuch für Geologie und Paläontologie 261: 177–193. https://doi.org/10.1127/0077-7749/2011/0159

Martin JE, Smith T, de Lapparent de Broin F, Escuillié F, Delfino M (2014) Late Palaeocene eusuchian remains from Mont de Berru, France, and the origin of the alligatoroid *Diplocynodon*. Zoological Journal of Linnean Society 172: 867–891. https://doi.org/10.1111/zoj.12195

Massone T, Böhme M (2022) Re-evaluation of the morphology and phylogeny of *Diplocynodon levantinicum* Huene & Nikoloff, 1963 and the stratigraphic age of the West Maritsa coal field (Upper Thrace Basin, Bulgaria). PeerJ 10: e14167. https://doi.org/10.7717/peerj.14167

Narváez I, de Celis A, Escaso F, De Jesús SM, Pérez-García A, Rodríguez A, Ortega F (2021) Redescription and phylogenetic placement of the Spanish middle Eocene eusuchian *Duerosuchus piscator* (Crocodylia, Planocraniidae). Journal of Vertebrate Paleontology 41. https://doi.org/10.1080/02724634.2021.1974868

Narváez I, de Celis A, Escaso F, Martín de Jesús S, Pérez-García A, Ortega F (2024) A new Crocodyloidea from the middle Eocene of Zamora (Duero Basin, Spain). Anatomical Record, 1–15. https://doi.org/10.1002/ar.25422

Ortega F, Armenteros I, de Celis A, Escaso F, Huerta P, Martín de Jesús S, Narváez I, Pérez-García A, Sanz JL (2020) Crocodyliformes and Testudines from the Eocene of the Duero Basin (northwestern Spain): an update of their diversity and stratigraphic context. Historical Biology 34: 1560–1581. https://doi.org/10.1080/08912963.2022.2051503

Piras P, Buscalioni A (2006) *Diplocynodon muelleri* comb. nov., an Oligocene diplocynodontine alligatoroid from Catalonia (Ebro Basin, Lleida province, Spain). Journal of Vertebrate Paleontology 26: 608–620. https://doi.org/10.1671/0272-4634(2006)26[608:DMCNAO]2.0.CO;2

Platt SG, Rainwater TR, Thorbjarnarson JB, Martin D (2011) Size estimation, morphometrics, sex ratio, sexual size dimorphism, and biomass of Crocodylus acutus in the coastal zone of Belize, Salamandra 47: 179–192. https://doi.org/10.18475/cjos.v45i1.a12

Puértolas-Pascual E, Serrano-Martínez A, Pérez-Pueyo M, Bádenas B, Canudo JI (2022) New data on the neuroanatomy of basal eusuchian crocodylomorphs (Allodaposuchidae) from the Upper Cretaceous of Spain. Cretaceous Research 135: 105170. https://doi.org/10.1016/j.cretres.2022.105170

Puértolas-Pascual E, Kuzmin IT, Serrano-Martínez A, Mateus O (2023) Neuroanatomy of the crocodylomorph *Portugalosuchus azenhae* from the Late Cretaceous of Portugal. Journal of Anatomy 242: 1–26. https://doi.org/10.1111/joa.1383

Rio JP, Mannion PD, Tschopp E, Martin JE, Delfino M (2020) Reappraisal of the morphology and phylogenetic relationships of the alligatoroid crocodylian *Diplocynodon hantoniensis* from the late Eocene of the United Kingdom. Zoological Journal of Linnean Society 188: 579–629. https://doi.org/10.1093/zoolinnean/zlz034

Schmitz L (2009) Quantitative estimates of visual performance features in fossil birds. Journal of Morphology 270: 759–773. https://doi.org/10.1002/jmor.10720

Serrano-Martínez A, Knoll F, Narváez I, Ortega F (2019a) Brain and pneumatic cavities of the braincase of the basal alligatoroid *Diplocynodon tormis* (Eocene, Spain). Journal of Vertebrate Paleontology 4634: e1572612. https://doi.org/10.1080/02724634.2019.1572612

Serrano-Martínez A, Knoll F, Narváez I, Lautenschlager S, Ortega F (2019b) Inner skull cavities of the basal eusuchian *Lohuecosuchus megadontos* (Upper Cretaceous, Spain) and neurosensorial implications. Cretaceous Research 93: 66–77. https://doi.org/10.1016/j.cretres.2018.08.016

Serrano-Martínez A, Knoll F, Narváez I, Lautenschlager S, Ortega F (2020) Neuroanatomical and neurosensorial analysis of the Late Cretaceous basal eusuchian *Agaresuchus fontisensis* (Cuenca, Spain). Papers in Palaeontology, 1–16. https://doi.org/10.1002/spp2.1296

Torres CR, Clarke JA (2018) Nocturnal giants: evolution of the sensory ecology in elephant birds and other palaeognaths inferred from digital brain reconstructions. Proceedings on Biological Sciences 285: 1–8. https://doi.org/10.1098/rspb.2018.1540

Venczel M, Codrea V (2022) A new late Eocene alligatoroid crocodyliform from Transylvania. C R Palevol 21: 411–429. https://doi.org/10.5852/cr-palevol2022v21a20

Watanabe A, Gignac PM, Balanoff AM, Green TL, Kley NJ, Norell MA (2018) Are endocasts good proxies for brain size and shape in archosaurs throughout ontogeny? Journal of Anatomy 234: 291–305. https://doi.org/10.1111/joa.12918

Webb GJW, Messel H (1978) Morphometric analysis of *Crocodylus porosus* from the north coast of Arnhem Land, Northern Australia. Australian Journal of Zoology 26: 1–27. https://doi.org/10.1071/ZO9780001

Weldon PJ, Ferguson MWJ (1993) Chemoreception in crocodylians: anatomy, natural history and empirical results. Brain, Behaviour and Evolution 41: 239–245. https://doi.org/10.1159/000113845

Weldon PJ, Swenson DJ, Olson JK, Brinkmeier WG (1990) The American alligator detects food chemicals in aquatic and terrestrial environments. Ethology 85: 191–198. https://doi.org/10.1111/j.1439-0310.1990.tb00399.x

Witmer LM, Ridgely RC (2008) The paranasal air sinuses of predatory and armored dinosaurs (Archosauria: Theropoda and Ankylosauria) and their contribution to cephalic structure. Anatomical Record 291: 1362–1388. https://doi.org/10.1002/ar.20794

Zelenitsky DK, Therrien F, Kobayashi Y (2009) Olfactory acuity in theropods: palaeobiological and evolutionary implications. Proceedings of the Royal Society B: Biological Sciences 276: 667–673. https://doi.org/10.1098/rspb.2008.1075

Zelenitsky DK, Therrien F, Ridgely RC, McGee AR, Witmer LM (2011) Evolution of olfaction in non-avian theropod dinosaurs and birds. Proceedings of the Royal Society B: Biological Sciences 278: 3625–3634. https://doi.org/10.1098/rspb.2011.0238